Chapter 4. SEMI-ENCLOSED SEAS, ISLANDS AND AUSTRALIA PAN-REGIONAL OVERVIEW (S)

TEMEL OGUZ

Middle East Technical University, Institute of Marine Sciences, Erdemli, Turkey

JILAN SU

Laboratory of Ocean Processes and Satellite Oceanography,
Second Institute of Oceanography, State Oceanic Administration, Hangzhou, China

Contents

1. Introduction

As a consequence of the flooding of the continental shelves by sea level rise at the end of the Last Glacial Period, the continents are surrounded today by shallow seas. Many of the inland seas, like the Baltic Sea, did not exist 10,000 years ago, or like the Black Sea have become filled with salty water while it was the largest fresh water body on Earth during the Pleistocene. The coastal seas are of prime interest to mankind since they contain a mosaic of complex and diverse ecosystems that involve rich natural resources and concentrated human activities, and provide a vital habitat for many commercial and endangered species. Their internal behavior affects their productivity, and they play an important role in the global cycle carbon, nitrogen and phosphorus because they receive massive inputs of these elements through anthropogenic sources and upwelling, exchange large amount of organic matter with the open oceans, and maintain productivity in higher trophic levels. In shallow water, nutrients are efficiently recycled many times, before becoming finally fixed in the sediments or being exported to the open ocean. There-

The Sea, Volume 14, edited by Allan R. Robinson and Kenneth H. Brink
ISBN 0–674–

fore, more productivity is maintained in the shallow and marginal seas than in most of the open ocean with positive effects on the harvest of fish and other marine species. A recent JGOFS synthesis indicated that the eutrophication-derived carbon deposit on the marginal seas partly compensate the missing anthropogenic CO_2 (Chen et al., 2004). As become highly eutrophic, the major problems today confronted with the marginal and shelf sea ecosystems are to assess types of possible structural changes possibly introduced by human-induced interventions in the next decades, to what extent they might be controlled, and implementation of possible strategies for sustainable use of their resources.

The semi-enclosed, marginal and shelf seas reviewed in this chapter as a part of the Pan-Regional overview of coastal oceans may be classified in terms of their morphological structures in three different groups: (i) nearly-enclosed basins with very limited exchanges with open oceans (e.g., the Baltic Sea, Mediterranean Sea, Black Sea, Red Sea, Arabian Gulf, Bohai Sea, Sea of Okhotsk, Japan/East Sea), (ii) partially-enclosed basins with moderate interactions with open oceans along their one or two boundaries (e.g., the North Sea, Yellow Sea, East China Sea, South China Sea), (iii) peripheral seas extending along continental margins and having strong interactions with open oceans along their two or three boundaries (e.g., the North Indian Ocean marginal seas, Outer Southeast Asia Sea, shelf seas around Australia and New Zealand). Aspects of the physical circulation, air-sea interactions and tides were overviewed by Church et al. (1998 – Vol. 11 The Sea). The overview presented in this chapter primarily focuses on their physical and ecosystem characteristics under four separate sections: (1) European semi-enclosed seas, (2) Arabian Peninsula and Northern Indian Ocean marginal seas, (3) East Asian (or Western North Pacific) marginal seas, (4) Australia-New Zealand shelf seas.

2. European semi-enclosed seas

2.1. Physical characteristics

The European marginal seas considered here include four semi-enclosed basins encircling the continental Europe. The Baltic Sea and the North Sea cover the western periphery, whereas the Mediterranean and the Black Seas encircle its southern-southeastern periphery (Fig. 4.1). The Baltic and North Seas (described in Rodhe et al., Chapter 26) are connected with each other by the Skagerak-Kattegat-Belt Sea region system where the Danish Straits constitute the shallowest and narrowest sections of the Baltic Sea with the deepest sill depth of about 18 m. The average depth of the entire Baltic Sea is about 60 m, and typical basin depths vary in the range 100 to 250 m. The North Sea is largely a shelf sea with an average depth about 100 m. It is connected to the North Atlantic along its northern and the southwestern boundaries. The Norwegian Trench, with a maximum depth of 700 m extends along the Norwegian coast.

The Baltic Sea reveals a fjord-type two-layer circulation. The restricted water exchange through the Danish straits, its long renewal time (about 30 years), and a comparatively large river discharges result in a very low mean salinity in the Baltic-Sea. The exchange of water through the Danish Straits, with low-saline outflows and high-saline inflows, is mainly forced by atmospheric events. The Baltic proper is strongly stratified by salinity. The surface salinity ranges from 8–9 in the south to 6–7 in the northern part of Baltic proper. A 50 to 70 m deep surface layer with no apparent vertical salinity gradient is separated from the weakly stratified deep water by a halocline. In addition, the surface layer becomes thermally stratified at a shallower depth in summer. The water in the deepest parts of the Baltic is renewed by infrequent, long-lasting extreme inflows through the Danish Straits. Except these periods of strong inflow the deep water is stagnant and eventually becomes anoxic. The frequency of these deep-water inflows has in fact decreased in recent decades, seemingly correlated with a pronounced positive North Atlantic Oscillation (NAO). Low salinity nature of the Baltic Sea results in the formation of sea ice every year. The entire Baltic Sea may be covered by ice during severe winters.

Figure 4.1 Location map and geographic setting of four semi-enclosed basins (The Baltic Sea, the North Sea, The Mediterranean Sea and The Black Sea) encircling the continental Europe.

In contrast, hydrographic conditions of the North Sea are characterized by a horizontal circulation system, stratified during the summer, with different dynamic regimes in its different regions. The North Sea is renewed rapidly on the order of one year. Most of the water enters from the northwestern boundary, circulates within the basin cyclonically, and flows out northward along the Norwegian Trench on the eastern side of the North Sea. Its average transport is around $2 \cdot 10^6$

$m^3 s^{-1}$. Relatively high salinity water also enters the North Sea through the British Channel, but at a far less transport rate. The salinity of the North Sea is close to 35. The central part of the North Sea is well-mixed vertically during winter and becomes stratified in summer due to heating. The tides are strong enough along the southern and western parts of the North Sea coasts to keep the water vertically mixed throughout the year, except near some river plumes. The Norwegian Trench region is stratified by salinity all year around due to the low salinity outflow, about 15 at the Kattegat, from the Baltic Sea and due to local river discharges. Kattegat is strongly stratified and its circulation is of estuarine type, i.e., entrainment of deep-water into the surface layer with an increasing surface-layer outflow along the Norwegian coast.

The Mediterranean Sea (Pinardi et al., Chapter 32) is separated from the Atlantic Ocean through the Strait of Gibraltar, and comprises the western and eastern basins, which are connected with each other through the Strait of Sicily. The eastern basin is further connected to the Aegean Sea with the several straits along the Cretan Sea and to the Black Sea through the Dardanelles and Bosphorus Straits. The basin depths are up to 4000–5000 m, but there are also extensive shelf areas. Pinardi et al. (Chapter 32) concentrates on six particular shelf regimes, three of which (the Gulf of Lions, the Northern Adriatic and the Egyptian shelves) are wide (>70 km) shelves and receive major river runoffs. Two other shelves along the Algerian and Israeli coasts are narrow (<30 km) shelves without significant runoff. The last one is the Sicily Strait that represents an extended shelf area without any relevant river input and is a large channel area for the exchange of water masses between the Eastern and Western Mediterranean sub-basins.

Difference in the many aspects of the physical characteristics between the northern and southern shelves is related to the Mediterranean precipitation regimes that result in zero runoff on the southern shores and river outflows on the northern shores. All the northern rivers have a spring maximum discharge connected to the ice-snow melting cycle and the precipitation maximum during winter. The noticeable exception is the Nile Delta, whose catchment basin extends further south to the tropical African wind belt and thus not regulated by the Mediterranean precipitation regime. Regulation by the Aswan Dam, however, has significantly reduced the Nile runoff.

The Mediterranean is a concentration basin, i.e. water losses exceed water gains from precipitation and runoff. In addition, the net heat budget of the basin is negative, so that the vertical thermohaline circulation is anti-estuarine, with waters exiting the Mediterranean at depths and entering from the Atlantic at the surface. The thermohaline circulation is of multi-decadal time scales with water mass formation in areas of the Northern Mediterranean. Both deep and intermediate waters form in the regions offshore the Gulf of Lions, the southern Adriatic and the northern Levantine basin, forced by intense heat losses during late winter (February-March) and influenced by the presence of a large scale cyclonic circulation driven by wind stress curl. The Aegean Sea has been a source of deep waters for the Ionian Sea abyssal plains during the eighties and first half of the nineties, but ceased to be so lately.

The sub-basin scale circulation has several time scales. The steady state component consists of permanent cyclonic and anticyclonic gyres that are wind-, and thermally-driven, superimposed to and interacting with the Gibraltar inflow system (Fig. 4.2 of Oguz et al., Chapter 33). These gyres induce open ocean upwelling and shelf area downwelling. The only large coastal upwelling centers are associated with wind driven permanent upwelling in the Sicilian and eastern Aegean coastal areas. These have a profound influence on the shelf scale ecosystem dynamics. The sub-basin scale structures have a seasonal amplitude associated with the large wind stress variability. Coupled to such a seasonal variability there is also a large signal of interannual variability. This implies that the general circulation structure can be quite different from the long-term mean and a more realistic picture of the sub-basin scale structures is presented in Fig. 4.4 of Oguz et al. (Chapter 33). The mesoscale circulation, pervasive in the basin, has by definition a shorter time scale, but the current amplitude can be large. In the Adriatic, evidence suggests that eddies are most frequent during spring and summer, when the atmospheric forcing relaxes.

The northern shelves are by and large Regions Of Freshwater Influence (ROFI) (Simpson, et al., 1991). The Rhone river plume moves cyclonically on the shelf and extends up to the westward side of the Gulf. During the winter, the shelf waters remain confined on the shelf while during the summer the Rhone plume and the shelf waters in general can extend offshore. The current system in this region is also dominated by the 30–50 km wide Liguro-Provencal-Catalan current (LPC). It flows along the edge of the continental shelf, but can form meanders penetrating the shelf, causing water exchange with the open sea 1000 times larger than the Rhône runoff. The shelf is dominated by transient mesoscale variability induced both by the LPC meandering and directly by the wind.

The dynamics of the narrow Algerian shelf are dominated by the Algerian current, which constitutes a part of the eastward flowing Gibraltar-Atlantic stream. Intense mesoscale features, such as eddy-dipole mushrooms, large meanders and eddies bring coastal water offshore and, at the same time, induce advection of nutrient-rich open ocean water on the shelf.

The circulation in the Sicily Strait has a two-layer system with a transport of 1–$2 \cdot 10^6\ m^3 s^{-1}$ in each layer and with strong seasonal variability. The Modified Atlantic Water (salinity lower than 38.2) flows across the whole Tunisian shelf in the southeastward direction and, about 200 m below, the Levantine Intermediate Water (LIW) flows in the opposite direction over the central trough. The Atlantic-Ionian Stream (AIS), a segment of the Gibraltar-Atlantic current system, enters the central Sicily Strait, forces upwelling on its northern side, especially during the summer when its current is strong. In addition, upwelling favorable winds are always present in this area. This current structure determines the high productivity of the region with rich spawning and nursing grounds.

The Adriatic Sea shelf area is controlled by air-sea fluxes and inflow of heat and salt at the shelf break. It is clearly a ROFI area influenced not only by the Po river but also by other northern Adriatic rivers discharging along the Italian side of the region. The Northern Adriatic is totally renewed every year, while the deep waters (200–250 m depth) in the middle basin renews locally only every few years. The deep waters of the Northern Adriatic are the heaviest in the Mediterranean and they slide southward, toward the Middle and the Southern Adriatic, and support the deep Mediterranean thermohaline circulation. The Po runoff is confined along the Italian coasts in winter but during the summer can reach across the Northern Adriatic, due to the stratification and the favorable winds. The other important driving mechanism is the winds: the Bora or easterly winds channeled through the Dinaric Alps and the Sirocco or southerly winds.

The Egyptian and Israelis shelf areas are opposite in extent but the latter is strongly inter-connected to the Egyptian slope current regime and to the sediment and biochemical fluxes of that region. The Egyptian shelf is still a ROFI area but very different from pre-Aswan dam period prior to 1968. The average annual discharge is only one-tenth of the value for the period prior to 1964 and the maximum discharge is now in winter. On the other hand, runoff is almost absent for the Israelis shelf. The eastward Nile Delta slope current is formed by the convergence of a southern branch of the Mid-Mediterranean Jet (MMJ). The slope current and the coastal current over the Egyptian shelf do not interact strongly because of the large extent of the shelf. The Israelis slope current is northward with large meanders and eddy detachment. It has strong influence on the coastal current on the Israeli shelf because of its narrow extent.

The Black Sea (Oguz et al., Chapter 33) has a flat abyssal plain with a maximum depth of around 2200 m. About 87% of the volume is anoxic. The northwestern shelf, occupying close to 20% of the total area, is the major shelf region with discharges from three of Europe's largest rivers: Danube, Dniepr and Dniestr. It communicates with the Aegean basin of the Mediterranean Sea through the Bosphorus and Dardanelles Straits. The Black Sea receives an inflow of about 9500m^3 s^{-1} of high salinity (~35) Mediterranean Sea water through the Bosphorus, which are balanced by the outflow through the Bosphorus of about 19,000m^3 s^{-1} of low salinity (~18) Black Sea water. Penetration of the Mediterranean water after the glacial period resulted in the development of a two-layer stratification by perhaps 8000 BP and gradual formation of the present day anoxic conditions in the lower layer.

Driven by both winds and buoyancy forces, the upper layer waters of the Black Sea are characterized by a predominantly cyclonic boundary current, the so-called Rim Current, flowing along the continental slope and a series of anticyclonic eddies on the shoreward side of the Rim Current. They evolve continuously by interactions among each other, as well as with meanders and filaments of the Rim Current. These mesoscale features evolving along the periphery of the basin apparently link coastal biogeochemical processes to those beyond the continental margin, even across the width of the basin to the coast on the other side. The interior circulation comprises several sub-basin scale gyres, each involving a series of cyclonic eddies. Over the northwestern shelf the circulation is dominated by the spreading of the Danube outflow. The coastal jet associated with the plume flows southward along the western coast. It is often unstable, exhibits meanders and spawns filaments, extending across the wide shelf zone.

The mixed layer changes seasonally, characterized by T~5–6°C, S~18.5–18.8 and a mixed-layer depth of up to 50 m depth in winter, and T~25°C, S~18 and a depth less than 20 m in summer. The intermediate and deep-water masses below the permanent halocline at depths of 100–150 m possess almost vertically uniform characteristics of T~9°C, S~22. The Mediterranean inflow, as following a north-northwestward track, mixes rapidly with the upper layer Black Sea water when crossing the shelf, flows down the slope with only slight differences of its temperature and salinity from those of the ambient waters. The residence time of the sinking plume of the Mediterranean inflow within the interior parts of the basin is ~400 years at 500 m. Below about 1700m, the entire abyssal water mass is uniform, formed as a result of convective mixing over several thousands of years driven by the bottom geothermal heat.

The upper layer water column was subjected to considerable climate-induced warming during the 1990s. The basin-averaged winter-mean (December-March) sea surface temperature (SST) was relatively uniform at 8.1±0.3°C from 1985 to 1991, followed by a strong cooling phase in 1992–1993 with the minimum SST value of 6.8°C, and subsequently an ~2°C rise in the SST by strong winter warming in 1994–1996. The winter warming continued at a more gradual level after 1996.

2.2. Ecosystem characteristics

The most distinguishing features of the European semi-enclosed seas are their limited exchanges with open ocean (except the North Sea), temperate climate, high level of nutrient content and eutrophication. They are generally among the most threatened marine ecosystems with great over-exploitation of commercial fish stocks, and endangered biotopes. Recently, there have been extensive efforts in all these seas to limit the algae production and reverse the development of eutrophication. About two-thirds of all nutrients causing eutrophication (nitrogen and phosphorus) in the Baltic, North and Black Seas come from land-based activities, including sewage, industrial and municipal waste and agricultural runoff. The overload of nutrients with respect to their consumption has made the algae production in the Baltic and Black Seas comparable to that of the North Sea, which is about 200 gC m^{-2} y^{-1} in offshore regions, and more than 300 gC m^{-2} y^{-1} in most coastal areas. The primary production is generally limited by nitrogen, but phosphorus might act as the major limited nutrients in some regions and/or some seasons. The phosphorus is particularly limits the production in the Mediterranean Sea. The Bothnian Bay is limited by phosphorus contrary to nitrogen limitation of the Baltic Proper. Similarly, major part of the North Sea is limited by nitrogen, except its southern part where the lack of sufficient phosphorus imposes constraint on the primary production. Silicate acts primary controller on the spring diatom bloom in the North Sea, and may regulate as well the annual succession of phytoplankters from diatoms to flagellates and dinoflagellates. The large-scale nutrient recycling predominates by vertical processes in the Baltic Sea, whereas the horizontal advection of nutrients has the first order importance in the North Sea. The Black Sea nutrient cycling, on the other hand, involve a mixture of these two effects; nutrients are advected by the Rim Current system around the periphery of the basin from the source region located along the northwestern coastal zone, distributed over the entire basin by mesoscale circulation system and recycled within the interior basin through very active biogeochemical pump in the water column (Oguz et al., Chapter 33). On the contrary, the Mediterranean Sea is regarded as an oligotrophic system with very poor biological production (less than 100 gC m^{-2} y^{-1}) except in some coastal regions. The Gulf of Lions (northwestern Mediterranean Sea), the Algerian coastal zone, the Northern Adriatic, the Nile Delta, and the northeastern part of the Levantine basin of the Eastern Mediterranean and the Northern Aegean Sea are identified as the most productive regions (Pinardi et al., Chapter 32). The oligotropy tends to be stronger towards east in the Mediterranean; the average phytoplankton biomass in the western Mediterranean is about three times higher than in the Eastern Mediterranean. Microbial loop constitutes a crucially important part of the lower trophic food web in all of these seas. The observations have been supported by the state-of-the-art ecosystem models capable of describing and predicting concentrations and fluxes of biologically important elements, providing new insight into the mechanisms of the functioning of the ecosystems, their temporal and spatial development, nutrient budgets, etc. An example for a recent review on ecological modeling studies for the North Sea is Moll and Radach (2003), and for the Black Sea in Oguz et al. (Chapter 33).

All the European sea ecosystems reveal the primary diatom-based phytoplankton bloom in the early-spring period immediately after the cessation of winter mixing and shallowing of the surface mixed layer. It is generally followed by a dinoflagellate-based bloom in the second part of the spring season. Following the nutrient depleted conditions in the surface mixed layer and formation of a weak, mixed subsurface phytoplankton production below the seasonal thermocline in summer period, the secondary bloom occurs in the autumn season. This classical annual phytoplankton structure varies to some extent in the southern and western coastal regions of the North Sea due to the presence of strong tidal currents. There, depending on water transparency and stratification, spring bloom might take place earlier, or be delayed until mid-summer, and therefore it is not possible to prescribe a characteristic seasonal cycle. On the other hand, in the region of Baltic outflow (i.e., the Danish Straits and the Kattegat) where the water column is stratified throughout the year, the spring bloom occurs early in the late winter (in early March) while the water is still cold (Rodhe et al., Chapter 26). This has also been a typical feature of the Black Sea spring bloom dynamics prior to mid-1990s, after which it has been altered as a result of strong decadal warming together with abrupt increases in the mean sea level and the net annual mean fresh water flux (Oguz et al., Chapter 33). The most notable impact of the climatic warming was to reduce upward nutrient supply from the nutricline due to less efficient vertical turbulent mixing and upwelling rate, and stronger stratification. From 1996 onwards, the major late winter-early spring peak of the classical annual phytoplankton biomass structure observed prior to mid-1990s was, therefore, either weakened or disappeared all together depending on local meteorological and oceanographic conditions during each of these years. The total annual phytoplankton biomass reduced by at least 100%. The effect of bottom-up limited unfavorable phytoplankton growth was reflected at higher trophic levels (e.g., mesozooplankton, gelatinous carnivores, and pelagic fishes) in terms of their reduced stocks.

A unique characteristic feature of the Baltic Sea and the Black Sea vertical biogeochemical structure is the depletion of oxygen at their deeper levels due to their utilization in the remineralization of sinking particulate matter. The sharp density stratification, accompanied with weak vertical circulation and mixing as well as limited lateral fluxes, inhibit ventilation of their sub-pycnocline waters from the surface. As a result, their vertical biogeochemical structures differ significantly from typical oceanic systems. The deep layer of the Black Sea became permanently anoxic within the last several thousand years, whereas the Baltic Sea is still able to renew itself occasionally. There, anoxia and hypoxia formation is only an intermittent process with some interannual variability depending on water turnover and vertical mixing characteristics and the amount of organic matter supplied from surface waters. The complex prey-predator interactions between different phytoplankton and zooplankton groups are tightly linked with very efficient remineralization – ammonification – nitrification – denitrification chain, and a series of different types, highly complex bacterially-mediated oxidation-reduction reactions controlling the structure and dynamics of the suboxic-anoxic transition zone. The efficiency of the remineralization process just below the euphotic layer leads to recycling of particulate matter many times in the water column before they are finally deposited at the bottom. In shallow areas, the sedimented organic matter is decomposed instead of burial as evident by low accumulation rate of organic matter in sediments in the Baltic Sea and the North Sea (Rodhe et al., Chapter 26).

In the Black Sea, and the Baltic Sea as well, the biogeochemical pump operates within the uppermost 100 m of the water column. The euphotic zone structure, covering maximally the uppermost ~50 m, is characterized by high oxygen concentrations on the order of 300 μM, and a year around biological activity. The underlying 20–30 m layer contains steep gradients in chemical properties where particle remineralization causes considerable reduction in oxygen concentration to the values of around 10 μM, whereas nitrate increases to maximum concentrations of 6–9 μM. The subsequent SubOxic Layer (SOL) of about 20–40 m is characterized by oxygen concentrations less than 10 μM, rapid decrease of nitrate concentrations to zero due to the consumption in organic matter decomposition. Denitrification therefore constitutes a major sink of nitrogen in these seas. Below the SOL, sulfate is used to decompose organic matter, and hydrogen sulfide is produced as a by-product. The loss to the deep anoxic layer is not more than 10% of the total particulate material remineralized, and is compensated by the riverine input. In the Black Sea, this highly delicate and efficient system maintains the current quasi-stable nature of the vertical biogeochemical structure, and thus preventing the upward rise of the sub-surface sulfidic waters. The anoxia has become more widespread and the anoxic periods more frequent, and the upper boundary of the SOL seems to have moved to shallower depth since 1960s. The interface between oxic and anoxic layers is the site of a series of complicated redox processes, which effectively prevent upward rise of hydrogen sulfide layer towards the surface layer (Oguz et al., Chapter 33).

In addition to human-induced interventions, ecosystem properties of the European seas exhibit a strong climatic modulation at interannual-to-interdecadal scales. For example, the oscillations and trends in the North Atlantic Oscillation (NAO) index have been reflected in the abundance and spatial distribution of plankton in the North Sea on time scales of decades (Fromentin and Planque, 1996). These variations were suggested to occur in response to change in physical characteristics of the water column (such as variations in the sea surface temperature, alterations in the stratification of the surface layer that modify the spring phytoplankton bloom), which are further modulated by the ecological and physiological properties of the plankton groups. Analysis of the plankton data from 1960 to 1995 indicated two particularly specific anomalous events during the late 1970s-early 1980s and the late 1980s-early 1990s. The first event, characterized by cold-boreal climate within the North Sea, was caused primarily by the unusual hydro-climatic conditions and a change in the overall North Atlantic circulation dynamics. An opposite situation of a warm oceanic climate took place a decade later giving rise to marked changes in three different trophic levels from 1988 onwards. These sharp changes have also been referred to as “regime shifts”. The North Sea regime shifts have been hypothesized to be the result of (i) a change in local hydrometeorological forcing, (ii) a displacement of oceanic biogeographical boundaries to the west of the European continental shelf, (iii) an increase in oceanic inflow into the North Sea. These features are apparently linked to each other, and have been influenced by common and large-scale climatological forcing (Beaugrand, 2004).

An examination of a wide spectrum of biogeochemical records from the Black Sea and the Baltic Sea also indicates similar robust interannual-to-interdecadal climate-induced fluctuations superimposed on the anthropogenic signal at all components of their ecosystem structures from nutrient concentrations to plankton biomass and pelagic fish stocks (Dippner et al., 2000; Mollmann et al., 2000, Daskalov, 2003; Oguz and Dippner, *in press*). They generally follow temporal variations of the physical properties, such as the upper layer temperature, salinity and sea level anomaly, in terms of their phases and durations. Synchronization of these physical-ecosystem variations with the North Atlantic Oscillation (NAO) index and its signature on the regional atmospheric properties (air temperature, wind stress magnitude, surface air pressure, evaporation minus precipitation) indicates a dominant role of the low frequency, large-scale climatic oscillations in these seas.

The drastic changes observed in the Black Sea ecosystem characteristics have occurred due to a combination of intense eutrophication (i.e., bottom-up control), trophic cascades induced by over-fishing and population outburst of gelatinous carnivores (i.e., top-down control), and decadal scale climatic fluctuations. These external factors have restructured the Black Sea ecosystem in the past few decades by first pronouncedly increasing nutrient concentration and plankton biomass, and small pelagic stock during the 1980s and then sharply decreasing in the 1990s. Over such linear trends of the anthropogenic signal, the entire hydro-meteorological, chemical and biological properties consistently present a robust natural climatic signal oscillating with the period of ~10 years. Whether or not the restructuring of the Black Sea occurs through regime shifts or more smooth changes is not clear, and requires further investigations.

The European sea ecosystems have also been characterized by significant changes in fish stocks during the last several decades due to climate-induced changes and effects of over-fishing. For example, the heavy unregulated fishing continued in the Black Sea during the early phase of the eutrophication (the early 1970s) led to the collapse of predator fish stocks (e.g., bonito, mackerel, bluefish, turbot, dolphin). By removal of large predators, smaller and lower valued planktivorous fishes (mainly anchovy and sprat) then started acting as the most abundant predator in the ecosystem. Their total stock alternates between high abundance of anchovy and sprat with ~5 year cycles, as seen in all other components of the ecosystem from nutrients through phytoplankton, mesozooplankton and higher predators. Periods of low sprat abundance were marked by high anchovy populations, or vise versa. Sprat dominated the total pelagic stock when the Black Sea was in its cooler regime, whereas anchovy’s control occurred in warmer years. Similarly, alternating herring and sardine stocks have been observed in the Baltic Sea on a decadal scale. They also appear to be related to hydrometeorological conditions, such as sea surface and air temperatures, duration of ice cover off Iceland, prevailing wind direction and the NAO. The years with severe winters are dominated by herring, whereas milder years are richer in terms of sardines. Similarly, the stock size of cod as a top predator in the Baltic ecosystem has attained its lowest level in the 1990s at the expense of increased stock of sprat (Kornilov et al., 2001).

3. Arabian Peninsula and Northern Indian Ocean marginal seas

3.1. Physical characteristics

The seas of the Arabian Peninsula (Richter and Abu-Hilal, Chapter 34) primarily include the Red Sea and Arabian Gulf, which are connected to the Arabian Sea through the Gulf of Aden and the Gulf of Oman, respectively (Fig. 4.2). On the eastern side of the peninsula is the shallow Arabian Gulf linked to the deep Gulf of Oman through the Strait of Hormuz. On the western side of the peninsula is the north-south oriented elongated deep trench of the Red Sea, which is connected to deep Gulf of Aden with a narrow and shallow entrance strait at Bab el Mandeb. These seas are important repositories of marine biodiversity and non-living resources, which contribute significantly to the economic, social and cultural prosperity of the region. The anthropogenic pressures are particularly damaging, as the extreme environmental regime of temperature and salinity already imposes natural stresses close to the physiological limits of the organisms.

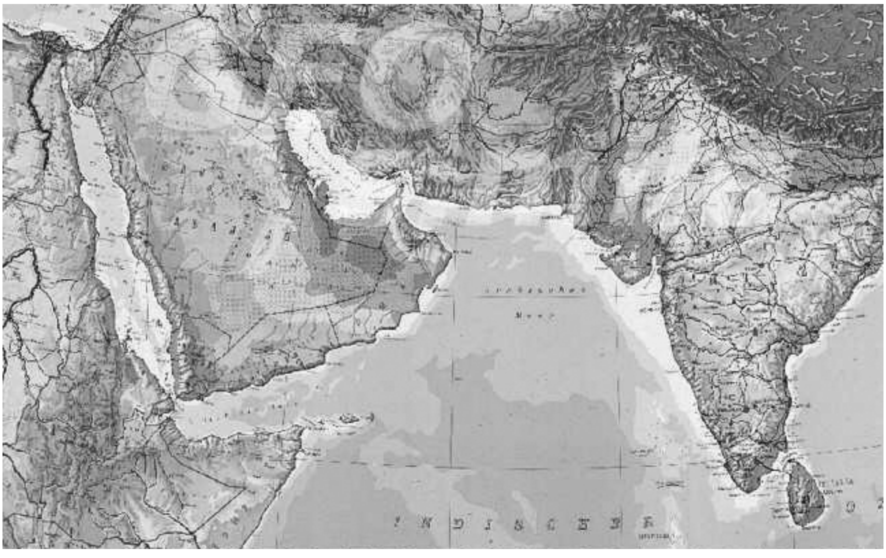

Figure 4.2 Location map and geographic setting of the seas of the Arabian Peninsula including the Red Sea, the Arabian Gulf and Arabian Sea. The Bay of Bengal is shown on the eastern side of the Indian sub-continent as well.

The Arabian Gulf is about 1000 km in length and has a mean depth of 35 m and a maximum depth less than 65 m. Estimates of renewal time for the Gulf vary between 2–5 years. The trough reaches 100 m across the Strait of Hormuz and deepens to more than 2000 m within 200 km of the Gulf of Oman. The Red Sea extends almost 2,000 km in NNW-SSE direction over an axial rift, with a maximum width of 354 km and a maximum depth of 2,850 m. The renewal time of the deep waters has been estimated at 30–45 years. A shallow sill-depth of 130 m, about 140 km north of the Strait of Bab el Mandeb, effectively cuts the Red Sea off from the cold deep waters of the world ocean. North of Port Sudan, the shelf narrows considerably, restricting coral reef development to the coastal fringes. The lack of river discharge, high evaporation and negligible rainfalls render the Red Sea one of the most saline waters in the ocean with salinity over 40.

The Arabian Monsoon is the dominant phenomenon affecting the oceanography of the region. It is most intense over the coastal Arabian Sea and southern Red Sea, while the northern Red Sea and Arabian Gulf are influenced more strongly by continental patterns. The winds and extreme aridity of the bordering lands enhance the evaporation rate around 2 m yr^{-1}. The resulting dense high salinity water masses drive a large-scale circulation in the marginal seas. Tidal currents are of first order importance in the Arabian Gulf, as well as the straits, but of second order in the Red Sea.

The persistent southward winds, the “Shamal”, in the northern half of the Arabian Gulf sets up a cyclonic circulation (Fig. 4.7), with westward current along the Iranian coast (upwelling) and eastward current along the Saudi and Emirates coasts (downwelling). The cyclonic circulation in the southern Gulf is driven by the surface water inflow through the Strait of Hormuz. The Saudi-Emirate coastal current appears to be enhanced by freshwater input from the Iraqi Shatt-al-Arab waterway. The surface water gains salt as it moves from the mouth (Strait of Hormuz) inwards and dense water formation occurs at a number of places in the shallow southern part of the Gulf. This water flows out below Indian Ocean surface water (IOSW) from the Gulf of Oman. A persistent thermal front across the Gulf close to Qatar appears related to the thermohaline exchange through the Hormuz Strait.

After transiting the Strait of Hormuz the Arabian Gulf deep water (PDW) cascades down slope into the Gulf of Oman, forming sub-mesoscale eddies (“Peddies”) as it moves toward the Indian Ocean. The surface outflow from the Arabian Gulf transits along the Emirate and Omani coast to the major promontory of Ras al Hadd. A major front and accompanying Ras al Hadd jet form at the collision of this Gulf outflow and the northeastward flowing Oman Coastal Current (OCC) along the southern Arabian margin (Fig. 4.9). The jet is highly variable and is believed to be at least $10 \cdot 10^6 m^3 s^{-1}$ during the SW monsoon. In the Gulf of Oman, there are seasonal, but inter-annually highly variable, upwelling areas along the coast of Iran.

The negative water balance due to excess evaporation drives an anti-estuarine circulation across Bab el Mandeb, with a surface inflow of comparatively fresh Gulf of Aden water into the Red Sea, and a bottom outflow of saline Red Sea water (RSW) over the sill into the Gulf of Aden (Fig. 4.10). The RSW, source of one of the most important intermediate water masses in the Indian Ocean, has an annual mean transport of $0.33 \cdot 10^6 m^3 s^{-1}$. In summer, the surface flow reverses beyond 17–18°N under the NNW winds and, consequently, the RSW also weakens significantly. The Suez Canal, completed in 1869, is insignificant in terms of the bulk volume flow, but non-negligible in terms of gene-flow of Red Sea biota into the Mediterranean.

The presence of a cyclonic gyre in the northern Red Sea is related to the formation of intermediate waters in winter. In the central Red Sea, two anti-cyclonic eddies are locked topographically near 18–19°N and 23–24°N. Non-permanent cyclonic and anti-cyclonic eddies in the southern Red Sea, associated with seasonally changing wind fields in this area, are related to the formation of intermediate waters. With velocities of up to more than 0.5 ms^{-1} these eddies override the ~0.1 ms^{-1} surface currents associated with the large-scale thermohaline circulation of the Red Sea.

The most important physical forcing over the North Indian Ocean (NIO) is the monsoon. The southern limit of monsoonal influence on oceanographic processes is approximately 10°S, which can be regarded as the natural southern boundary of the NIO. Rapid meridional changes in hydrochemical characteristics occur all along this boundary, called the Hydrochemical Front, which is maintained by the year-round, unidirectional (westward) South Equatorial Current. North of the Hydrochemical Front, the surface circulation in the NIO reverses every six months. The summer or southwest monsoon (SWM) period, from June to September, is more energetic than the winter or northeast monsoon (NEM) period, from December to February. It is also more energetic in the Northwest Indian Ocean (NWIO) than in the Northeast Indian Ocean (NEIO). Thus, strong seasonal upwelling occurs in the NWIO.

The balance between evaporation (E), precipitation (P) and runoff (R) also exhibits large geographical variability. With E-P exceeding 1 m y^{-1}, the northwestern Arabian Sea experiences the most arid conditions with surface salinity over 37. Along the southwest coast of India, intense SWM rainfall leads to an excess of precipitation over runoff within a belt a few hundred kilometers wide. In the Bay of Bengal, on the other hand, E-P decreases from slightly positive values along the southeast Indian coast to <-1 m y^{-1} over a wide area in the northeastern Bay and the Andaman Sea. Moreover, almost all major rivers of South Asia drain into the Bay of Bengal and the Andaman Sea, bringing in ~1.65 x 10^{12} m^3y^{-1} of freshwater. All these result in the rather low surface salinity (<30) in the northeastern Bay of Bengal.

The NIO is located within the tropical belt where changes in monsoon winds generate coastal and equatorial Kelvin waves and equatorial Rossby waves. Having both annual and sub-annual periods, these waves can propagate rapidly across the region, strongly influencing circulation over narrow shelves along the way. In areas where the shelf is wide, its circulation may be decoupled from large-scale processes, and factors such as tides, and local runoff may play a more important role in driving its currents.

Coastal circulation along Somalia is the most energetic during the SWM. The northward Somali Current has a volume transport comparable to that of the Gulf Stream. It is distinguished by the existence of several quasi-stationary anticyclonic eddies, inducing upwelling around 4° and 10°N. Further north, strong SWM monsoon winds also force intense upwelling along the coasts of Yemen and Oman. Predominate meso-scale eddies there facilitate rapid offshore advection of the cold upwelled water, as filaments and plumes, up to 1,000 km from the coast. Surface flow along the western boundary of the Arabian Sea including the southwestward flowing Somali Current is much weaker during the NEM. Further south the Kenyan coast experiences upwelling of less magnitude and receives significantly more runoff than the coasts farther north in the western Arabian Sea.

Circulation along the eastern shores of the Arabian Sea is less organized during the SWM when the winds are strongest than during the NEM when the winds are quite light. During the SWM, upwelling induced by the southward West Indian Coastal Current (WICC) is masked by the presence of a warm, low-salinity lens formed as a result of large land runoff and precipitation. During the NEM, the WICC flows toward the north and carries almost twice as much water as its summer variant in spite of the unfavourable winds. It causes downwelling all along the west coast of India.

The upper layers along the east and west coasts of India are dynamically linked through circulation around the island of Sri Lanka. This link is particularly strong during the NEM when the equatorward East Indian Coastal Current feeds the westbound Northeast Monsoon Current. During the SWM the enormous freshwater discharge significantly affects surface circulation as it spreads around altering properties of surface waters.

Available information on oceanographic processes along the coastal strip stretching from Bangladesh in the north to Indonesia in the south is extremely scarce. Outside the continental shelf in the Andaman Sea, water characteristics below the sill depth (~1.3 km) are remarkably uniform and very similar to those in the Bay of Bengal, including the O_2 concentration, suggesting rapid renewal of their deep water.

3.2. Ecosystem characteristics

The pelagic production in the seas around the Arabian Peninsula exhibits large spatial and temporal differences depending on the rate of supply of nutrients due to large scale monsoonal wind forcing and associated upwelling in coastal areas, in the Gulf of Aden, Arabian margin and the Iranian coast of the Gulf of Oman, convective mixing in the northern and shallow areas of the Red Sea and the Arabian Gulf, as well as fronts and straits controls (Richter and Abu-Hilal, Chapter 34). Nitrogen usually limits the productivity, and iron acts as a micronutrient controlling the productivity in monsoonal upwelling areas. The biological productivity in the Red Sea is generally poor, and oligotrophy becomes more persistent and stronger towards north. The lack of anthropogenic nutrient load, restricted inflow of nutrients from the Arabian Sea across the narrow and shallow straits of Bab el Mandeb, as well as strong vertical stratification, which limits the supply of new nutrients from below, are the major causes for the development of rather unproductive conditions, except some reefs along its margins and shelves in the southern part of the Red Sea. The deposition of dust transported from the nearby sources and subsequent biological fixation of N_2 acts as an additional source of nutrient in the region. Observations in the Gulf of Aqaba, Red Sea (Fig. 17, Richter and Abu-Hilal, Chapter 34) indicated that more than 95% of the photosynthetic biomass is dominated by ultraphytoplankton species such as *Cryptophyte* and *Chlorophyte* in winter months, blue-green *Synechococcus* in spring, and *Prochlorococcus* in summer. The development of diazotrophic filamentous blue-green *Trichodesmium* in summer and early fall is also observed. The small size of the phototrophs at the base of the food chain, therefore, renders a large part of the primary production, which is however unavailable to the classical food chain via copepods and pelagic fish. The bulk of the energy is dissipated in the microbial loop of picophytoplankton-heterotrophic nanoflagellates-ciliates before reaching higher trophic levels. As a result, pelagic fish stocks are low in the Red Sea.

The productivity may be enhanced locally and temporally below the seasonal thermocline during SWM winds (June to September) as a result of advection of nutrient rich subsurface waters into the Red Sea. The production might be similarly enhanced within the surface layer by the advection of surface waters from the Gulf of Aden during NE monsoon period (December to February). The NEM winds mixes upper layer water column by means of wind and buoyancy (cooling)-induced mixing, and thus gives rise to large phytoplankton blooms on either side of Bab el Mandeb during winter. The Arabian Gulf is more productive water body with respect to the Red Sea, but its productivity is about an order of magnitude lower than the Arabian Sea, except upwelling-induced high production in the Gulf of Oman. Both the Red Sea and the Arabian Gulf ecosystems are limited by nitrogen. However, phosphorus stress may ultimately govern the final successional stages of production in the Red Sea (Richter and Abu-Hilal, Chapter 34). On the other hand, silicate does not play a major role on the primary productivity.

The shallow coastal zones of Arabian Gulf and the Red Sea support extensive sea grass meadows and algal beds providing important feeding and breeding habitats for many types of marine organisms such as pearl oysters, shrimps and green turtles. Salt marshes and mangroves are important intertidal habitats along the coasts of the Arabian Peninsula providing nurseries for marine fish and invertebrates and refuges and breeding areas for marine and terrestrial wildlife. The Arabian Gulf and Red Sea also include rich and highly diverse reef ecosystems distributed primarily along the coasts of Saudi Arabia, Kuwait, Bahrain and Qatar. These reefs, however, have experienced high frequency recurrences of bleaching during the last decade due to gradual rising of sea surface temperatures (Richter and Abu-Hilal, Chapter 34).

The upwelling area along the eastern coast of the Gulf of Aden and Omanian coastal zone reveals one of the richest and unexploited potential fishing ground in the world. Two subsequent strong and long-lasting phytoplankton blooms developed in response to intense coastal upwelling generated by strong alongshore winds during the SWM periods provide continual food supply for zooplankton productivity, and support large pelagic fisheries. The phytoplankton biomass, immediately grazed by the dominant copepod species, is then channeled efficiently to the higher trophic levels.

A strong pattern of seasonality in biological production driven by monsoonal dynamics is more clearly evident in the Arabian Sea by extensive phytoplankton blooms develop during both monsoon periods. During the SWM period, prominent phytoplankton blooms are developed during August-September along the Omani coast in response to strong upwelling-induced nutrient accumulation within the surface layer. The nutrients are upwelled from depths of 100–200 m, and exceed concentrations of 20 μM for nitrate and 1.5 μM for phosphate. Concentrations of micronutrients such as iron (Fe) are also high enough not to limit primary production. The highest phytoplankton biomass and primary production are observed along the coast with primary production and chlorophyll concentration values as high as ~3 gC m^{-2} d^{-1} and ~15 mg m^{-3}. These elevated values may be extended several 100 km offshore (i.e. interior of the western Arabian Sea) due primarily to eastward advection of upwelled waters within the Somali Current and local wind-forced vertical entrainment linked to deepening of the mixed layer. The filaments and other forms of mesoscale structures of the coastal current system also contribute to nutrient enhancement of offshore waters. The nitrate and phosphate concentrations in open north-central Arabian Sea increase up to 4–6 μM and 0.6–0.8 μM, respectively, during the periods of active convection. The observations further indicate the role of physiological adaptation of the offshore communities to higher irradiances for maintaining relatively high productivity in offshore areas. The phytoplankton community is dominated in a greater proportion by picoplankton and other small forms (Richter and Abu-Hilal, Chapter 34).

The second peak of seasonal phytoplankton biomass structure occurs during winter (January-February). The cool, dry northerlies that characterize the NEM result in a typical wintertime convection and subsequent nutrient enrichment in the northern Arabian Sea. The convective mixing is further promoted by increases in the salinity of surface waters due to evaporative cooling. The solar heating of the surface waters during the day inhibits the convection to some extent, and generates large-magnitude diurnal oscillations in the mixed layer depth. This mechanism was shown to lead to high rates of primary production (~1–2 gC m^{-2} d^{-1}) and an accumulation of phytoplankton biomass over the course of the NEM as the nitrate is accumulated slowly in the surface mixed layer. The nitrate stored in the surface layer is not utilized completely as a result of the combined impact of zooplankton grazing and the mixed layer's diurnal cycling. The diurnal mixing further homogenizes the physical and biogeochemical properties down to the seasonal thermocline, which lies deeper than the base of the euphotic zone, and thus provides a continual supply of plant material subject to remineralization in the subeuphotic zone.

The sediment trap measurements carried out off Somalia and Oman showed a strong link between monsoons and particle production and sedimentation. The bimodal biological production in the surface layer of the water column was inferred from these measurements by the primary and secondary maxima of particle flux in the SWM and NEM periods, respectively. The material undergoing sedimentation after the onset of the SWM production contained more carbonate than opal initially, indicating the dominance of coccolithophores and insufficient supply of silicate to support diatom growth. As silicate supply went up later during the season and thus diatoms became more abundant, opal dominated content of the sinking material. The likely reason for lower export flux during NEM relative to SWM is limitation of diatom productivity due to lower silicate concentrations in surface waters. More organic matter is thus retained in the surface productive layer in the form of dissolved pool to support the new production as well as growth of heterotrophic bacteria as observed the subsequent spring intermonsoon season. Heterotrophic bacteria along with picophytoplankton may, in turn, sustain microzooplankton growth and give rise to an efficient microbial loop in the Arabian Sea.

The mechanism of nutrient supply to the euphotic zone in the eastern Arabian Sea (i.e. western coast of the Indian Subcontinent), on the other hand, differs somewhat. During the SWM, upwelling along the Indian coast is to a large extent driven by remote forcing and linked to the large-scale circulation system rather than the coastal upwelling driven by local winds as in the Somalian coast of the western Arabian Sea. Therefore, nutrients are upwelled into a much narrower coastal zone in the eastern Arabian Sea. Due to the presence of low-density surface waters, upwelling can not usually penetrate up to the surface, and spread offshore as in the western Arabian Sea. Thus, nitrate concentration in the thin surface layer is close to the detection limit, but increases abruptly to values around 20 μM just within the lower part of the euphotic zone. The resulting subsurface production is around ~6 gC m^{-2} d^{-1} which is much higher than anywhere in the Arabian Sea. On the other hand, non-upwelling conditions during the NEM and the spring intermonsoon season lead to strong oligotrophy in the eastern Arabian Sea. Instead, these waters with warm SST, stable water column stratification, low fixed nitrogen but appreciable phosphate concentrations as well as adequate supply of micronutrients from the nearby land as well as from subsurface levels offer an ideal environment for the growth of *trichodesmium*.

A distinguishing feature of the Red Sea-Arabian Sea-Arabian Gulf ecosystems is the presence of mesopelagic oxygen minimum zone (OMZ), characterized by oxygen concentrations less than 10 μM, at intermediate depths with its core around 400–500 m (Richter and Abu-Hilal, Chapter 34). The OMZ is caused by utilization of oxygen in the process of organic matter degradation at intermediate depths as described in the previous section for the Black and Baltic Seas. The core of the oxygen minimum zone approximately lies at a density level of ~26.6 σ. within the more saline Arabian Gulf water. The oxygen deficiency of the water masses entering the Arabian Sea around the tip of India and/or from the Southern Ocean as well as weak aeration from a lack of an opening to the north are additional factors for impoverished oxygen content at the intermediate waters of the Arabian Sea. The bottom of the oxygen minimum zone roughly coincides with the characteristic density (~27.2 σ.) of high salinity Red Sea water residing approximately at the depth of 750 m. The OMZ has a spatially variable structure, showing greatest oxygen deficiency in the northern basin. This region is further characterized by intense denitrification process as suggested by a local increase in nitrite concentrations of more than 1.0 μM. The oxygen-deficient zone at shallower depths also appears within the eastern Arabian Sea shelf waters. All these features of the OMZ resemble very closely the oxygen depletion zones of the Baltic and Black Seas which are all characterized by the lack of ventilation of their intermediate layers through oxygen-rich open ocean waters, as well as efficient organic matter production and remineralization through the nitrification – ammonification – denitrification chain of the biogeochemical cycle.

The Bay of Bengal receives high riverine input, particularly by Ganges/Brahmaputra Rivers. They import considerable nutrient and lithogenic matter into the Bay with considerable seasonal and interannual variations under monsoonal dynamics. Lateral supply of nutrients and lithogenic matter from the shelf regions are particularly high (>300 mg m^{-2} d^{-1}) in the central Bay of Bengal during NEM. When riverine input and the offshore propagation of the river plume is reduced during SWM, the advection from an upwelling area along the east coast of India during NE-SW intermonsoon season becomes the most dominant control mechanism. The conditions promoting biological production in coastal waters of the Bay of Bengal are less efficient with respect to those of the Arabian Sea. The loss of a major portion of the nutrients supplied by rivers to the deep basin across the narrow shelf zone along the periphery of the Bay limits the production in coastal and shelf waters. The SWM winds may induce upwelling along the eastern coast of the Indian subcontinent, but this mechanism can only enrich lower part of the euphotic zone while the near-surface levels of the water column remain to be depleted in nutrients. They thus promote subsurface productivity and chlorophyll maximum similar to those observed in the Arabian Sea during spring intermonsoonal season (March-April). Primary production typically attains the values of ~0.5 gC m^{-2} d^{-1}. On the other hand, the surface waters are cooled during the NEM period to a very similar extent as in the Arabian Sea, but less efficient cross-pycnocline mixing due to stronger stratification (as a result of lower mixed layer salinities by about 2) limits introduction of new nutrients into the euphotic zone. Once again, the near-surface levels remain to be depleted by nutrients and thus unproductive. The primary production in the water column is lower than that occurred during the SEM. The available information on biogeochemistry of the eastern part of the Bay of Bengal stretching from Bangladesh in the north to Indonesia in the south is, on the other hand, extremely scarce.

The uniformly high particulate organic carbon flux in deep waters of the Bay of Bengal is attributed to the ballasting effect of lithogenic minerals. Their aggregation into sinking biogenic particles increases the sinking speed of the aggregates, which leads to relatively lower oxygen consumption in the deep waters of the Bay of Bengal, and more deposition into the sediments. Consequently, the OMZ is appreciably thinner, and less vigorous denitrification takes places as compared to the Arabian Sea.

4. East Asian (or Western North Pacific) marginal seas

4.1. Physical characteristics

The rim of the Northwest Pacific Sea, extending latitudinally from 60ºN to the tropics, embraces six contiguous but distinct marginal seas (Fig. 4.3). The northernmost component of this system comprises the Sea of Okhotsk and the Japan/East Sea, which are described in Zhang et al., (Zhang et al., Chapter 16). Further south is covered by four regional seas surrounding China: the Bohai Sea, the Yellow Sea, the East China Sea, and the South China Sea. Their physical and ecosystem characteristics are presented in Zhang and Su (Zhang and Su, Chapter 17). The characteristics of the Outer Southeast Asia Seas (OSEAS) spread between Indochina Peninsula and Australia are given in Liu et al. (Liu et al., Chapter 18).

The Sea of Okhotsk has an average depth of 821 m and a maximum depth of 3916 m in Kurile Basin in the south. Its shelves, mostly in the north and northeast, account for almost 40% of the total area. The average and the maximum depths of the Japan/East Sea (hereafter referred to as JES) basin are about 1,350 m and 3,700 m, respectively. The Sea of Okhotsk and JES are connected through two shallow and narrow straits, the 40 km wide La Pérouse Strait (also called Soya Strait) with a sill-depth of 40 m and the Tartar Strait with a sill-depth of 10 m and a choke-width less than 10 km. The Sea of Okhotsk is connected to the Pacific

Ocean through tens of Kurile straits, totaling over 500 km in width. The JES is connected to the East China Sea through the Korea Strait of ~200 km in width and a sill-depth of 140m, and to the subarctic Pacific through the Tsugaru Strait of ~20 km in width and a sill-depth of 130m.

The Okhotsk Sea is icebound from November to June, with maximal coverage in March except in areas near the Kamchatka and Kurile Islands. Winter cooling over the northern shelf produces the Cold Intermediate Layer (CIL) with a core of (–2°C, 32.8–33.5), which remains below the seasonal thermocline in most part of the sea during the warm season. Presence of CIL is important for the productivity of the sea. The warmer and saltier intermediate water mass lies below the CIL. Mixing of the Okhotsk Sea and Pacific water in the Kurile Basin during winter results in the North Pacific Intermediate Water (NPIW).

Four water masses identified in the JES are called by the Surface Water above 150 m, the Intermediate Water in the depth range of 150–500 m, the Deep Water between the depths of 500 and 2,000 m, and the Bottom Water below 2,000 m. The three cold water masses beneath the permanent thermocline, all formed locally, are renewed through stronger deep mixing accompanied with strong winter cooling off the southern coast of Russia in multi-decadal scale.

Driven by the winds and water exchange with the Pacific, the Sea of Okhotsk is characterized by a large-scale cyclonic gyre with two major meridional flows, namely, the northward West Kamchatka Current bringing in the Pacific water and the southward East Sakhalin Current (Fig. 16.5). Downwelling of relatively warm waters shoreward of the West Kamchatka Current is vital for the many temperate boreal species inhabiting in the region. Numerous mesoscale eddies (up to 200 km in diameter) are observed in the boundary of the large-scale gyre system. Small-scale eddies up to 20–30 km in diameter, important for fisheries, are observed in the offshore and coastal regions, likely related to tide-topography interaction.

In the early 1990s, the West Kamchatka Current slackens with the lessening of water exchange with the Pacific through the northern Kurile straits. Accompanying this decrease was the intensification of water exchange with the JES. Instead of moving southerly in the traditional way, the intensified Soya Current turned northward. The normal cyclonic circulation in the very southern part of the Sea of Okhotsk was replaced by an anticyclonic one.

The JES receives from the East China Sea (ECS), through the Korea Strait, a flow rate of about $2 \cdot 10^6$ m^3s^{-1} in winter and $3.5 \cdot 10^6$ m^3s^{-1} in summer, (ECS) water. Transport out of the JES includes $2 \cdot 10^6$ m^3s^{-1} and $3 \cdot 10^6$ m^3s^{-1} to the Pacific in winter and summer, respectively, through the Tsugaru Strait, and a 0.5–$1 \cdot 10^6$ m^3s^{-1} to the Sea of Okhotsk in summer. This through flow in the JES is called the Tsushima Warm Current (TWC). TWC has three branches, one the East Korean Warm Current flowing northwards as a planetary western boundary current and then eastward from the coast along the polar front near 40°N, and the other two branches flowing along the slope offshore of and the coast of Honshu, respectively. A wind- and density-induced cyclonic gyre is found in the northwestern part of the TWC. The southwestward western boundary current of this gyre is called the Liman Cold Current.

Figure 4.3 Location map and geographic setting of the East Asian marginal Seas extending along north-south direction from the Okhotsk Sea, Japan/East Sea, Bohai-Yellow Seas, East China Sea, South China Sea as well as the Outer Southeast Asia Sea further south.

The oceanographic regimes in the China Seas change from semi-enclosed shallow water region to the epi-abyssal basin with vast shelf seas in between. The Bohai Sea (BS) and the Yellow Sea (YS) are rather shallow, with average depths of 18 and 44 m respectively. The East China Sea (ECS) has an extensive shelf; the presence of the Okinawa Trough increases its average depth to 370 m. The South China Sea (SCS) is characterized by a deep basin with maximum depth of 5,500 m and an average depth of 1,350 m. The renewal time of the four regional seas ranges from 1–2 yr for the BS to 40–50 yr for the SCS.

Circulation in the China Seas is strongly affected by the monsoon winds and the Kuroshio. Surges of cold and dry northerly winds prevail in winter, and southerly monsoon and frequent typhoons dominate in summer. Wind excited sub-tidal sea-level fluctuations propagate southward along the coast of China to the SCS. Effects of the monsoon and the Kuroshio intrusion have resulted in various circulation regimes and different water masses in the China Seas, with important consequence on the biogeochemical cycles. Additionally, the monsoon system plays an important role in delivering land-based materials to the China Seas.

Dynamically, the BS and YS can be regarded as one semi-enclosed shallow sea. In winter the YS is well-mixed vertically and the wind-induced northward advection of warm water balances the heat loss to the atmosphere. In summer, large area of the sea is stratified due to heating of the surface water, with the remnant cold winter water staying in the lower layer. Tidal fronts border the stratified area. There is a depletion of freshwater in the BS due to excessive evaporation and reduced river discharge, resulting in the slow increase of its average salinity.

The ECS is one of the large shelf regions of the world and is noted for its high primary productivity. It receives a tremendous riverine supply of freshwater, carrying terrigenous suspended sediment and nutrients from land-sources. The total riverine load of water amounts to 1200 $km^3\ yr^{-1}$, of which the Changjiang (Yangtse River) accounts for 90–95 %. Off the shelf break, the Kuroshio moves northward with a water transport of ca. $25–30 \cdot 10^6\ m^3\ s^{-1}$. The Kuroshio and its branches (e.g. Taiwan Warm Current and Tsushima Current) over the ECS shelf have important effects on the circulation in this region. The Taiwan Warm Current is composed of waters from both the northward flow through Taiwan Strait and the shelf-intrusion waters from Kuroshio, especially at area north of Taiwan. It occupies a significant part of the ECS and sustains coastal upwelling, enhanced from the southerly winds in summer, along the ECS coast. Extensive exchange of water and nutrients between the ECS and the Kuroshio occurs across the shelf break region through upwelling and frontal processes.

The SCS is a Mediterranean-type basin dominated by monsoon processes. The surface area of SCS is more than two times larger than the sum of BS, YS and ECS. It comprises of a wide range of ecosystems, including the shelf, coral reefs, upwelling region and deep basin. Through the Luzon Strait, the Philippine Sea is the only important source of open ocean water for the SCS. However, the hydrographic properties of the two systems have distinctive features in the vertical profiles. Exchange of waters between Philippine Sea and SCS is rather complicated and far from well understood, especially the way the Kuroshio Waters enter the South China Sea. The bottom water in the SCS Proper reveals considerable uniformity with salinity of 34.6 and potential temperature of 2.1°C, similar to the deep water of the Philippine Sea.

The basin-wide SCS circulation, principally wind-driven, is dominated by a cyclonic gyre in winter and a north-south cyclonic-anticyclonic pair in summer. Significant offshore upwelling can be found east of the Vietnam coast in summer, affecting an area of ca. 1500–2000 km^2. Coastal upwelling is an important oceanographic feature of the SCS when the summer monsoon prevails, particularly in the north and west. The upwelling system is characterized by an increase in surface salinity of 2–4 and a decrease in temperature of 1–5°C, compared with adjacent open SCS waters. The shelf regions are well developed in the northern and western parts of the SCS, particularly off the large river mouths (e.g. Pearl River Estuary and Mekong Delta). They have water depth of 200–250 m and extend seaward over a distance of 300–400 km.

The Outer South-East Asia Seas (OSEAS), spread between the Indochina Peninsula and Australia, are inter-connected water bodies with extremely varied morphology, ranging from shallow shelves and coral reefs to deep basins and enclosed bays. The excessive rainfall (2–4 m yr^{-1}) in the western part of this region and the extremely high sediment yield on many of the islands and peninsulas distinguish this area as an exceptionally strong source region of geochemical input to the ocean. The so-called Wallace's Line divides the Asiatic fauna from the Australian fauna. This OSEAS region is adjacent to the SCS proper to the northwest, the Philippine Sea to the northeast and the Indian Ocean to the south. The massive western Pacific warm pool sits just to the east and the return flow of the global conveyer belt from the Pacific to the Indian Ocean, namely, the Indonesian throughflow, passes though the deep channels inside the region. Consequently, the physical and biogeochemical states of the OSEAS are potentially sensitive to climate changes.

The topographic features in the region are quite complex, reflecting its tectonic history. The seas to the west and south of the biggest island, Borneo, including the Gulf of Thailand, the Sunda Shelf, and the Java Sea, are all quite shallow (<75 m), whereas those to the east, including the Sulu, Sulawesi (also known as Celebes), Maluku (also known as Molucca) and Banda Seas, are all quite deep (>1000 m). The transition occurs at a line along the western boundaries of the Makassar and the Lombok Straits.

The semi-enclosed Gulf of Thailand is separated from the SCS by a sill-depth of about 40 m, while the Sunda Shelf and its extensions connect the SCS with the Indian Ocean through a series of shallow seas. The Sulu Sea connects with the SCS over a sill-depth of 420 m and its connection with the Philippine Sea has an effective sill-depth of only 110 m. The Maluku Sea is connected to the Philippine Sea through an effective sill-depth of 2340 m. Its connection to the Flores Sea to the south via the Makassar Strait is through an effective sill depth of 550 m. The Banda and the Flores Seas are connected to the Indian Ocean through a series of passages, with effective sill-depths ranging between 300 m (Lombok Strait) and 1250 m (Timor Strait).

The climate in this region is primarily driven by the Southeast Asian monsoons. Monsoon related rainfall in this region contributes 15–20% of the freshwater runoff in the world. From November to March the stronger northeast monsoon (NEM) blows over the South China Sea and turns into the northwest monsoon (NWM) over Java, Flores and Banda Seas south of the Equator. The moisture-laden NWM results in heavy rains in the eastern OSEAS. From June to September the southeast monsoon (SEM) originates from the Southern Hemisphere high-pressure belt and is relatively dry and cool over the eastern OSEAS. Further north, it turns into the southwest monsoon (SWM) as it passes the Equator and picks up more water vapor along the way. Being in the outskirt of the Southeast Asian monsoon, climatological winds over the Indonesian Seas and Gulf of Thailand are considerably weaker.

Water renewal in the Gulf of Thailand and the Sulu Sea is mainly through exchange with the SCS. The penetration of the SCS water into the Sulu Sea occurs in late summer and the flow reverses in winter. By contrast, the Sulu Sea water flows into the Sulawesi Sea all year round. Intrusion of the low salinity water originating from the SCS is evident near the Lombok Strait under the NWM in February. Replacement of the deep Banda Sea water by the Pacific Ocean water is estimated to be around 40 years. The surface outflow to the Indian Ocean is dominated by water from the North Pacific, whereas the deep outflow through the Timor and Ombai Straits is significantly fed by waters from the South Pacific.

The complex topography and the high frequency forcing of the monsoons, including monsoon related precipitation, result in strong modification of the water mass properties. The average temperature and salinity distribution (Fig. 18.6) illustrate some of the dominant hydrographic features in this region. The variation of rainfall causes strong seasonal variation of salinity in the OSEAS, while the temperature remain consistently high (mostly around 28°C) throughout the year. Low salinity water extends from the Gulf of Thailand to Sunda Shelf, Java Sea and Flores Sea. High salinity water ($S>34.5$) occurs off northern Australia, where the climate is relatively arid, and off northern New Guinea, where the sea surface temperature is very high.

The Gulf of Thailand is less than 100 m deep but the water mass is well stratified throughout the year. In boreal winter, there is a strong surface inflow along the western coast of the Gulf, creating a weak anticyclonic surface circulation, and most of the return flow to the SCS is via the bottom layer. In boreal summer, the surface water has a net outward flow, compensated by the net inflow of bottom water.

Seasonal reversal of surface circulation occurs throughout most of the Indonesian Seas, with an eastward surface current from November to March and a westward flow from May to September. Reversal of zonal currents generates on the eastern end of the Banda Sea upwelling in boreal summer and downwelling in boreal winter. Driven remotely by circulation and sea level gradients beyond regional scale, there is a strong southward surface current in boreal summer but likely a weak northward one in boreal winter in the Makassar Strait.

4.2. Ecosystem characteristics

The rim of the Northwest Pacific is among the most populous regions in the world. It inhabits almost 2 billion people, 60% of whom are concentrated in coastal areas. In the past several decades, the region has been the center of considerable economic growth, which brought increasing urbanization and, consequently, human-induced stresses on the ecosystem and exploitation of marine living resources. In addition to those provided in Chapters 16, 17 and 18, a detailed assessment of the present state of these marine ecosystems has been given by the North Pacific Marine Science Organization (PICES) Report (2004).

This collection of marginal sea ecosystems, extending from 60°N to the tropics, reveals temporally varying chemical and biological characteristics from the periods of seasonal to interdecadal. It also comprises the world's richest marine diversity, and produces approximately 40% of the global fish catch. The high biological productivity prevails in the northern (subarctic) latitudes, whereas oligotrophy dominates towards south. The nutrient supply to the photosynthetic layer by intense vertical mixing, upwelling and river runoff drives a strong spring production, whereas the recycling is responsible for most of the production during rest of the year. The inflow of nutrient rich waters across straits connecting these seas with each other and with the open waters of the Pacific Ocean further contribute to the nutrient enrichment. For example, the Kuroshio affects the South China Sea through the Luzon Strait and then intrudes the East China Sea across the broad shelf. The effect of anthropogenic nutrient supply as well as monsoon winds and tides are other dominant factors controlling the annual nutrient budget in shallow basins, like the Bohai and East China Seas.

Bi-modal annual phytoplankton structure with two main blooms in spring and autumn is observed in the Sea of Okhotsk and other East Asian Seas, which is the similar structure to that described earlier for the European marginal seas. The Okhotsk Sea spring phytoplankton bloom structure (in April-June) is dominated by the cold-water diatom species, while nanophytoplankton prevails more predominantly in the summer (Zhang et al., Chapter 16). The autumn phytoplankton bloom, which takes places during the mixed layer deepening phase in September to December, is mostly dominated by coccolithophorids under the conditions of low nutrients, high solar radiation and mixed layer temperatures of about 15°C. The estimate of total annual primary production varies within the range of 260–350 gC m^{-2} y^{-1}. The high end of this range constitutes one of the highest in the entire northwest Pacific. About 50% of the total annual primary production is associated with the spring season, although there are only few time series to show the interannual variations in the intensity and timing of the phytoplankton blooms and primary production.

Efficient recycling and high rate of organic matter decomposition also constitute a significant part of total primary production in the Okhotsk Sea. Nutrient recycling is further enhanced by mesoscale eddies. Observations (Zhang et al., Chapter 16) indicated that cyclones enrich the surface layer with nutrients by upwelling, while anticyclones pump organic material into deeper layers promoting the development of the heterotrophic fauna. Photosynthesis and decomposition occur most intensively within the anticyclones where waters accumulate from adjacent area and sink down.

Extremely high productivity has always been a characteristic feature of the Okhotsk Sea throughout the last Glacial Maximum and much of the Holocene. Following a decline in productivity during 11,000 and 10,000 years ago during Younger Dryas cooling, the warming triggered intensive diatom production, opal accumulation and a strong oxygen deficiency which led to significant changes in the benthic fauna assemblages from ~5000 to present. Today, the Okhotsk Sea involves enormous reservoirs of CH_4, CO_2, H_2S, dissolved trace components, as well as the highest rate of methane production in the Northern Hemisphere.

In the Japan/East Sea (JES), the annual primary production is roughly comparable to that in the Okhotsk Sea, but its seasonal cycle differs in its cold (northwestern) and warm (southeastern) sectors. The spring bloom initiates in February and reaches its maximum intensity in April in the southern sector. The spring production then continues in the northern cold-water region in May, where low vertical stability of the water column prevents earlier bloom formation. As in the Okhotsk Sea, the spring bloom constitutes half of the annual production, the rest is shared almost equally by the summer and autumn blooms. The ecosystem characteristics of the lower trophic food web in JES have recently been investigated by the prototype model named NEMURO (North Pacific Ecosystem Model for Understanding Regional Oceanography). The early version of the model has 11 prognostic variables: two groups of phytoplankton (large and small), three groups of zooplankton (small, large predatory), inorganic nitrogen (nitrate and ammonium), particulate and dissolved organic nitrogen, particulate organic silicate, and silicate concentration. The model has later been extended to include a simplified carbonate cycle (Yamanaka et al., 2004), and the microbial loop (PICES, 2003).

The ecosystem characteristics of the Bohai Sea, the Yellow Sea, the East China Sea and the South China Sea, forming four components of China Seas, are strongly linked to the dynamical processes associated with the monsoonal winds, Kuroshio and tides (Zhang and Su, Chapter 17). The anthropogenic perturbation and surface nutrient concentrations fall from Bohai-Yellow Seas in the north to South China Sea in the south. In terms of both horizontal and vertical gradients, the northern part of the China Seas possesses more variability throughout the year, whereas the conditions in the South China Sea are more typical of open-ocean conditions with more stable and temporally uniform vertical structures. The Kuroshio's effect is most notably seen in the South and East China Seas, whereas monsoon primarily controls the production in the South China Sea. Tidal effects are predominantly felt in the open shelf waters of the East China Sea. Anthropogenic nutrient supply from Huanghe and Changjiang Rivers introduces enhanced production in coastal waters. Except these coastal waters, the annual primary production in the China Sea is generally low: decreasing from 150–200 gC m^{-2} y^{-1} in the Yellow and East China Seas to 50–100 gC m^{-2} y^{-1} in the South China Sea. The high eutrophication introduces high rate of primary production in coastal regions of the Bohai Sea, which reduces toward its central and outer parts where low level of nutrient concentrations persists throughout the year due to rapid exchanges with the offshore waters. The oligotrophy becomes more dominant in the Yellow Sea receiving very limited nutrient input from rivers as well as from the open ocean, except for the period from the late autumn to early spring, when the nutrients are supplied from the subsurface levels by increased vertical mixing. The major part of the annual primary production occurs during spring, which is ~5 times stronger than the autumn production.

The exchange with the Kuroshio along its open boundary and the discharge of the Changjiang River along the coast introduce a rich variety of ecosystem conditions in the East China Sea (Zhang and Su, Chapter 17). The amount of nutrients supplied by Kuroshio across the shelf break region through upwelling and frontal exchanges is about 5 times more than supplied from the inner shelf. The Kuroshio Subsurface Waters have relatively high phosphorus and silicate and compensate deficiency of these nutrients supplied anthropogenically. The depth integrated primary production is around ~300–400 mgC m^{-2} d^{-1}, on the average, along the coastal zone and mid-shelf during spring and summer due to the favorable temperatures, higher light intensities. Further offshore in the Kuroshio region, primary production decreases two-to-four fold. The corresponding surface chlorophyll concentrations in summer span from 5–10 mg m^{-3} in the coastal zone to 1–2 mg m^{-3} in broad shelf zone, and to 0.1–0.2 mg m^{-3} within the Kuroshio region. The autotrophic production is immediately followed by enhanced heterotrophic activities as suggested by high ciliates abundance and maximal bacterial growth rates in summer.

The South China Sea involves various different kinds of ecosystems, spanning from coral reefs with very efficient nutrient cycling within a rather closed environment to wetlands (e.g. mangrove), estuaries, highly productive coastal upwelling regions (e.g. off the Vietnam coast) induced by the summer monsoons, and wide shelf regions shelf and deep-basin systems (Zhang and Su, Chapter 17). The coastal upwelling occurs in response to southerly monsoon winds in summer, and results in enhancement of nitrate along the Vietnam coast up to ~20 μM which is twice the corresponding values further interior. Likewise, phosphate concentration goes up to 1.0–1.5 μM, which is almost 5 times higher than that of the open sea value. The subsequent changes in the surface production are monitored by the 10-fold increase in the satellite chlorophyll retrieval to 5–10 mg m^{-3}. Anthropogenic nutrients supplied by rivers also lead to appreciable production along the northern and western parts identified by the surface chlorophyll concentration of ~2 mg m^{-3} and depth integrated primary production up to 500 mgC m^{-2} d^{-1}. It is generally phosphorus limited due to high rate of nitrate input from land-base sources, whereas the situation reverses within the broad shelf region away from the coastal zone. Further offshore, in the South China Sea Proper, the depth integrated production is characterized by 50–100 gC m^{-2} y^{-1}, which is 2–3 times lower than the reported for the shelf, and 5–10 times lower than that of coral reefs located in the central and southern parts of the East China Sea. The South China Sea Proper reflects a Mediterranean character with strong oligotrophy, and limited contribution from the land-based sources.

The OSEAS cover the tropical longitude band between 100°E to 140°E with most extensive continental shelves in the world. By virtue of the year-around high solar radiation and river discharges, they provide approximately 20–40% of productivity in tropics with great diversity, although it represents only ~10% of the trophical band (Liu et al., Chapter 18). The OSEAS also comprises the most magnificent and diverse coral reef systems in the world. On the other hand, its deeper basins, like the Sulu, Sulawesi and Banda Seas, reflect characteristics of the deep ocean ecosystems with very narrow shelves and margins.

The monsoonal winds control the production in the shelves and deep basins in the OSEAS. The SWM regime, by generating upwelling along the western coast of the Gulf of Tailand, triggers diatom and dinoflagellate production. During SEM, production increases in the eastern seas. Under the NEM, upwelling generates phytoplankton growth along the Vietnamese coast and the eastern coast of Peninsular Malay. During the NWM, on the other hand, oligotrophic conditions prevail, with clear waters and low nutrient concentrations. The production is supported mainly by regenerated nutrients, and cyanobacteria, protozoans dominate the system. In the Sulawesi and Flores Seas, average primary production was shown to become double when the wind was switched from NWM to SEM.

The observational data and budget calculations for the Western North Pacific marginal seas suggest that a small fraction of carbon (~15%) is exported across the shelf-break in dissolved and particulate organic form, and a small amount deposited in the sediments. The net offshore export is mostly supported by upwelling. Majority of the production is thus regenerated locally on the shelves (Liu et al., 2003). These marginal seas, like for the European shelves, are mostly undersaturated with respect to atmospheric CO_2 in the surface layer mainly as a result of the biological pump and winter cooling. The air-to-sea flux of CO_2 is around 1.1 ± 0.3 mol C m^{-2} yr^{-1} (Chen et al., 2004). The denitrification loss through release of N_2 is $\sim 0.07 \pm 0.3$ mol C m^{-2} yr^{-1}. The Western North Pacific marginal seas may have taken up 1.6 ± 0.3 Gt (10^{15} g) of excess carbon, of which approximately 50% is supported by the South China Sea, 20% by the Japan/East Sea, 11% by the Okhotsk Sea, 13% by the Bering Sea and 4% by the Yellow and East China Seas.

The East Asian Seas exhibited a broad range of impacts of climate forcing from plankton to fishes and seabirds. The changes in the ecosystem properties was triggered both from lower to higher trophic levels (bottom-up forcing) and by altering distribution, abundance and growth of lower trophic levels through the changes in top predators (top-down control). The most dramatic changes (the so-called regime shifts) emerged in the form of rapid and sharp changes in regional ecosystems and abiotic environments (e.g., the Pacific Decadal Oscillation (PDO), Sea Surface Temperature (SST), zooplankton abundance, and commercial fish distributions) to the north of 20°N. On a decadal time scale, four distinct climatic regime shifts or deviations from normal climatic patterns, the so-called Pacific Decadal Oscillations, have occurred during the last century. Each of these regime shifts has been followed by either a warm or a cold phase lasting for about 25–30 years until the next transition cycle. The transitions occurred in the mid-1920s, mid-1940s, mid-1970s and mid-1990s.

The 1976–1977 regime shift phenomenon was the most profoundly studied event among them. It was caused by intensification of the North Pacific High and the subartic Aleutian Low pressure systems. These changes led to enlargement of the subtropical gyre and increased volume transport of the Kuroshio Current, and subsequently intrusion of warmer waters into the East/Japan Sea as well as southern part of the Sea of Okhotsk, which are thus characterized by relatively higher temperatures in the surface layer of the water column. As the low pressure system was intensified, the precipitation were also increased, winds became stronger resulting ultimately in deeper mixed layers, lower spring chlorophyll concentration associated with weaker primary production. Accordingly, zooplankton biomass showed a sharp decline after the regime shift. These changes were reflected to higher trophic levels as an increase in the warm water fish (sardine and filefish) catches until the late 1980s at the expense of the depletion of cold water fish (saury, anchovy) stocks. Further north, in the Sea of Okhotsk, walleye pollock stock was replaced by herring for the same reason. These changes persisted until 1988, and then system reverted back to the pre-1976 conditions characterized by increased primary and secondary productions with higher phytoplankton and zooplankton biomass, collapse of recruitment, biomass and production of sardine while those of mackerel increased substantially.

According to the observations (Rebstock and Kang, 2003), the responses of the East Asian marginal seas to the 1989 climatic regime shift have not been similar. This implies that, in 1989, they have reverted back to somewhat different ecosystem states due to timing of the responses rather than differences in biological properties. The regime shifts have been traced, most notably, in the form of pronounced changes in fish stocks and catches during the late 1980s and early 1990s. For example, squid has replaced saury, cod and walleye Pollock. Recruitment and biomass as well as catch of mackerel increased, while sardine declined at this time. Some of these trends reversed changes that occurred in the mid-1970s, when Pollock replaced sandfish and sardines replaced saury. The 1976–1977 regime shift phenomenon was further evaluated, and the changes observed were supported quantitatively by model simulations. In particular, using a three-dimensional coupled physical-biological model, Chai et al. (2003) have provided the dynamical linkages between large-scale physical processes and the smaller-scale biological responses in the North Pacific and associated 1976–1977 regime shift event. Exploring the trophodynamic interactions between the lower and higher trophic levels in response to long-term climate-induced changes are currently underway by combining the NEMURO lower trophic level food web model with the ECOPATH/ECOSIM higher trophic food web model (PICES, 2003).

In addition to abrupt regime shifts, there are some indications of gradual transformation of the water column biogeochemical structure under the impacts of climate and/or human-induced perturbations. The spring phytoplankton biomass in the Japan/East Sea declined during the 1980s because of warming and intensification of the stratification of the upper layer water column. The tendency towards a decrease in oxygen and an increase in temperature of the intermediate-bottom waters of the Okhotsk Sea has been reported due to warming and a reduction or cessation of new bottom water mass formation. As the temperature has been increasing and oxygen concentration has been decreasing, the depth of the oxygen minimum layer has been increasing since the 1950s. Persistence of these conditions may lead to anoxia in the bottom waters of the Japan/East Sea within the next few hundreds of years.

5. Australia-New Zealand shelf seas

5.1. Physical characteristics

Australia is an island continent extending from tropical to mid-latitude waters, bounded by three oceans (Pacific, Indian and Southern) and four marginal seas (the Timor, Arafura, Coral, and Tasman Seas; Fig. 4.4). The Australia's Shelf Seas (Condie and Harris, Chapter 35) are exposed to climatological conditions ranging from the westerly Roaring Forties winds in the south, to monsoon and tropical cyclone conditions in the north. It also encompasses regions of extreme biodiversity, with 80 percent of southern temperate species endemic to the region.

Australia's shelves are highly variable in terms of their widths and profiles. The width ranges from about 10 km offshore from Fraser Island to over 500 km at the Arafura Shelf. Most of Australia's shelves are relatively smooth, but some parts are rimmed by shelf edge barrier reef systems. They also span a number of climatic zones, ranging from wet tropics in the northeast and dry tropics in the northwest to temperate conditions in the south.

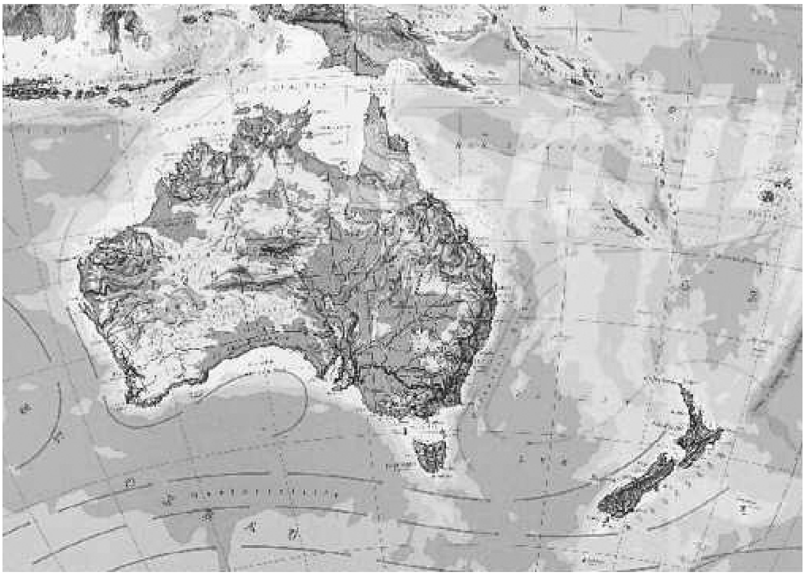

Figure 4.4 Location map and geographic setting of the marginal seas around Australia and New Zealand. They involve the Timor Sea, Arafura Sea, Tasman Sea as well as Australian shelf seas encircled by the Indian, Pacific and Southern Oceans.

The large-scale wind patterns over Australia and its seas are influenced by the tropical monsoon in the north, where persistent southeasterly trade winds are replaced by northwesterlies during summer. The trade winds extend over the subtropics and are replaced by the westerly Roaring Forties during winter and spring. Wind-driven circulation is significant over much of shelf seas and is known to generate coastally-trapped waves around the coastline. Except for the southwestern Australia, significant wind-driven upwelling events tend to be infrequent and localized. On the other hand, stronger winds and surface cooling during winter months often results in complete vertical mixing within shallow regions such as the Gulf of Carpentaria and Bass Strait.

The East Australian Current is the major western boundary current in the South Pacific, fed from the east by a complex pattern of flows forming the South Equatorial Current. Moving south, it develops a series of intense anticyclonic eddies, carrying warm low-nutrient water southward. It separates from the upper slope at around 33^{o}S to join the southern boundary of the South Pacific subtropical gyre. On the west coast, the poleward flowing Leeuwin Current intensifies along the upper continental slope, carrying warm, low-salinity water southward. It opposes the prevailing southerly winds, effectively preventing the formation of a major upwelling system like those observed off the west coasts of other continents. From autumn and on the Leeuwin Current wraps around the southwest corner of the continent, and flows eastward across the Great Australian Bight, forming a rather long continual coastal current.

Another major current system coincides with the Subtropical Front south of Australia. It separates the high nutrient waters of the Subantarctic Zone from more depleted subtropical waters. It is also evident in the mixed layer depth distribution, but tends to be smeared out in the seasonal temperature and salinity fields due to variability in the location of the frontal zone. During most of the year the Subtropical Front is south of the Australian continent, but tends to encroach onto the Tasmanian continental slope during the winter months.

The islands of New Zealand rise from a submerged continental block, split by a NE–SW running plate boundary, stretching from 18°S to 56°S (Fig. 4.4). New Zealand's four major coastal environments, namely, the northeast shelf of North Island, Greater Cook Strait, western South Island shelf and Otago shelf are described in Bradford-Grieve et al., Chapter 36. New Zealand has as a wide range of combinations of physical and climatic features that influence river flow regimes. The wettest areas of the country are on the western slopes of the Southern Alps where average rainfall is greater than 6.4 m y^{-1}, and the driest are in central Otago. Semidiurnal tides, as counterclockwise traveling coastally-trapped Kelvin waves, have a complete 360° range of phase around New Zealand. The tides are always 180° out of phase through Cook Strait, resulting in very high tidal velocities through the strait. High tidal velocities also occur north of Cape Reinga and in Foveaux Strait.

After separating from the coast of Australia, the East Australian Current crosses the Tasman Sea forming the Tasman Front. A portion of it forms the East Auckland Current along the northeast continental shelf break of New Zealand, with a mean transport of $9 \cdot 10^6$ m^3s^{-1}. Most of this flow deflects south around the eastern coast of the North Island before forming the northern side of the Subtropical Front (STF). Three permanent eddies lie offshore of this boundary current (Fig. 4.1). The western side of the STF passes around the South Island and has an associated current along the east coast of the South Island, called the Southland Current, with an average transport of around $8 \cdot 10^6$ m^3s^{-1}. These offshore currents are particularly important in inducing shelf edge currents and oceanic eddies that maintain an intimate contact of oceanic waters with the coastal zone.

Circulation on the northeastern shelf of North Island is wind-forced, with upwelling and downwelling being the dominant signals. Much of the shelf is less than 40 km wide and the proximity of slope waters has significant implications for the inner shelf and coastal zone physics and nutrient supply. It is one of the most productive shelf regions of New Zealand.

The Greater Cook Strait is exposed to strong westerly winds, strong tidal currents, and moderate freshwater input. Its most conspicuous feature in summer is the Kahurangi upwelling plume driven by the westerly winds. This upwelling results in a north-eastwards shedding of cold, nutrient-rich water that is associated with greater concentrations of chlorophyll than those in the surrounding waters.

The western South Island shelf is flanked by a nearby, high mountain range and has a width ranging from 25 to 100 km. It receives high freshwater input and riverine sediments, and is exposed to prevailing westerly winds. The continental slope off this region is an important breeding ground of hoki that forms New Zealand's largest fishery. Coastal currents are highly variable although the mean alongshore flow is weak. At subtidal frequencies the coastally-trapped wave is the dominant signal in the shelf currents and is generated by the broad-band wind-forced variable flow through Cook Strait. Rivers contribute a relatively large proportion of the shelf water volume, modifying the shelf salinity distribution.

Driven by the Southland Current, the narrow Otago shelf is dominated by northward along-shelf flow of subtropical origin and a meso-scale lee eddy north of Otago Peninsula. The unusual close proximity to the STF facilitates the introduction of distinctive subantarctic elements to the biota. Modern sedimentation is low and confined to an inner shelf sand wedge. Relict and biogenic sediments dominate the middle and outer shelf and provide for a well-developed sessile epifauna.

5.2. *Ecosystem characteristics*

Australia and New Zealand are generally considered to be strongly oligotrophic, as in most trophic systems. Due to limited anthropogenic input, nutrients are generally supplied to the surface layer by wind-driven upwelling events, which are however irregular, short-lived and localized. Strong winds and surface cooling in some parts of Australia (e.g., Bass Strait near the southeastern corner, Gulf of Carpentaria along the northern coast) during winter months might promote longer-term nutrient enhancement in the surface mixed layer. Therefore, the southeastern part of the Australia shelf seas is highly productive (primary productivity >300 gC $m^{-2} y^{-1}$), rich in marine habitat with many species endemic to Australia, and characterizes one of the most diverse soft-bottom benthic communities in the world (Condie and Harris, Chapter 35). The nutrients are supplied by runoff from Murray-Darling River system as well as wind-induced mixing associated with seasonal storms events. The productivity gradually decreases towards the northern sector of the relatively narrow (<50 km) east-Australian shelf, without any appreciable large seasonal phytoplankton blooms and organic matter production (primary productivity ~150 gC m^{-2} y^{-1}). The region is adversely affected by the southward transport of low-nutrient tropical waters in the East Australian Current system. Further north of the east-Australian shelf includes the Great Barrier Reef, which is the largest system of corals and related life forms along the Australia's 2000 km-long northeast coast. The nutrient enrichment and mixing in the region are essentially due to tidal dynamics as well as riverine inputs with strong peaks during floods induced by tropical cyclones. Moreover, local current and wind systems along this coast do not promote productive upwelling episodes. Thus, in general, total phytoplankton productivity is relatively low, and does not follow a regular seasonal cycle. The productivity becomes even lower within the Northwest Australian shelf further west. The lack of intrusion of nutrient rich slope waters onto the shelf further than 50 m isobath imposes further limitation on the local production, in addition to limited nutrient input due to tidal motion, coastal upwelling and terrestrial input.

Contrary to the low surface biological activity, the shelves along the northern coast of Australia exhibit high habitat diversity and complexity (Condie and Harris, Chapter 35). They support a remarkably wide spectrum of marine fauna, including tropical fish, turtles, dugongs, whales, hard and soft corals, sponges, and many crustaceans. The food chain is supported by enhanced subsurface productivity, and includes a range of commercial species, even though their stocks are quite small and confined to the coral atolls at the edge of the shelf zone. The tropic shelf ecosystem is primarily driven by a predator, the Crown-of-Thorns starfish (*Acanthaster planci),* coral-eating echiderm that has devastated reefs. Their occasional outbreaks introduce a major impact on the reef ecosystems, which typically recover on time-scales of 20 years or more.

Further south, along the west coast, the ecosystem shifts from trophic to mid-latitude character encompassing diverse pelagic and coastal ecosystems. The production is also poor but may tend to enhance locally by upwelling especially near the southwest corner. The Leeuwin Current is responsible for larval advection and recruitment of tropical fishes to the south. Its most dramatic contribution to the western Australian shelf ecosystem is however to suppress upwelling along the coast and thus resulting low biological productivity in trophic levels.

The New Zealand shelf ecosystems, extending about 30 degrees latitude from the subtropics in the north to the sub-Antarctic region in the south, are mainly characterized by its temperate climate. The marine environment is very diverse and includes estuaries, mudflats, mangroves, seagrass, reefs, deep-sea trenches, etc (Bradford-Grieve et al., Chapter 36). The nutrient concentrations also exhibit strong latitudinal gradient with nitrate concentrations at 200 m off the east coast shelf break changing from 10 mmol m^{-3} in the northeast to 16 mmol m^{-3} in the southeast. The nutrient concentrations are more uniform in the western shelf waters. The phytoplankton annual structure reveals a typical temperate basin character with a successive diatom and picophytoplankton blooms in the spring, and a weak bloom in the autumn. The biomass in terms of chlorophyll exceeds 2.0 mg m^{-3} in spring. Winter mixing and spring upwelling cause nutrient enrichment and elevated phytoplankton growth predominantly within the northeastern shelf. The remineralized nutrients and continuing supply of new nutrient from off-shelf by means of upwelling sustain the shelf production in the early summer until the upwelling is switched to the downwelling regime. Primary production both in the Northeast shelf and the narrow Otago shelf in the southeast is estimated around 150–200 gC m^{-2} y^{-1} for the neritic to subtropical zone and somewhat lower for further offshore. On the other hand, within the Western South Island Shelf, biological productivity is relatively weaker and the highest concentrations of chlorophyll, primary production, and zooplankton biomass are usually confined into a narrow band along the coast both in summer and winter. This is because of the weaker upwelling, which often does not have surface expression and is overlaid by brackish waters of the river origin.

Australia and New Zealand's coral reefs are among the region's most sensitive environments to climate change—through potential inundation, flooding, erosion, saline intrusion, bleaching and death of corals, and possible changes in tropical cyclone occurrence. Climate change impacts will be compounded by the rapid growth in environmental stresses arising from existing population growth and increasing tourism. Coral bleaching is associated with several factors (including extreme temperatures and solar irradiance, subaerial exposure, sedimentation, freshwater dilution, contaminants, and diseases) acting singly or in combination. This occurs when sea temperatures rise more than 2°C above normal, which is often associated with ENSO episodes. Harmful effect of warm waters, however, may be occasionally compensated by cyclones, which may cool surface temperatures within few days by mixing with deep water.

6. Conclusions

The overview chapter presented here is concluded by a brief summary of achievements toward more comprehensive understanding of the physical- biogeochemical processes, regulatory roles of human effects and modes of natural variability on the ecosystem functioning of coastal, marginal, semi-enclosed and shelf seas. The intense and concentrated field efforts realized during the last decade within the framework of national and international, interdisciplinary research programs, further supported by satellite data and sophisticated modeling initiatives, provided a basis to address a series of contemporary scientific issues. First, they have clearly demonstrated a broad spectrum of variability in time, space and complexity of these ecosystems, contrary to our earlier perception of their ecological steady state, and more simplified view of the food web structure. Significant variations in nutrients and biological properties have been noted in association with mesoscale features of the boundary currents, and eddy-dominated circulation systems. These features often modulate two-way exchange between coastal and offshore waters and lead to very efficient material transport. It became also evident that the food web structures, when profoundly affected by internal and external factors associated with natural and anthropogenic changes, may undergo strong nonlinear changes within its existing state or may abruptly switch to another state with almost no warning of impending changes. Parallel to increasing human stresses, the eutrophication-induced alterations in biogeochemical cycles and transformations of carbon, nitrogen, phosphorus, sulphur and other trace elements have been consistently identified in most of the regions included in the present overview. The most striking modification was identification of highly efficient nutrient recycling and increasing contribution of microbial loop to the lower trophic food web structure. The important role of coastal and marginal seas in the global carbon cycle is also more clearly quantified. Rich biological activity enables to uptake of atmospheric CO_2 and transfers it to the open ocean through the continental shelf pump or exports to the deep ocean. Today, an exciting and challenging scientific research theme is to build up an interdisciplinary modeling framework through process-oriented model explorations and data assimilations which may hopefully allow soon to forecast biological changes resulting from natural and/or anthropogenic perturbations, and to assess the extent to which undesirable changes can be ameliorated and damaged communities are restored.

Bibliography

Beaugrand, G., 2004. The North Sea regime shift: evidence, causes, mechanisms and consequences. *Progr. Oceanogr.,* **60,** 245–262.

Chai, F., M. Jiang, R. T. Barber, R. C. Dugdale, Y. Chao, 2003. Interdecadal variation of the transition zone chlorophyll front : A physical-biological model simulation between 1960 and 1990. *J. Oceanogr.,* **59,** 461–475.

Chen, A.C, A. Andreev, K-R. Kim, and M. Yamamoto, 2004. Roles of continental shelves and marginal seas in the biogeochemical cycles of the North Pacific Ocean. *J. Oceanogr.,* **60,** 17–44.

Daskalov G. M., 2003. Long-term changes in fish abundance and environmental indices in the Black Sea. *Mar. Ecol. Prog. Ser.,* **255,** 259–270.

Dippner, J.W., G. Kornilovs, and L. Sidrevich, 2000. Long-term variability of zooplankton in the Central Baltic Sea. *J. Mar. Syst.,* **25,** 23–31.

Fromentin, J.M. and B. Planque, 1996. *Calanus* and environment in the eastern North Atlantic. 2. Influence of the North Atlantic Oscillation on *Calanus finmarchicus* and *C. hegolandicus. Mar. Ecol. Prog. Ser.,* **143,** 111–118.

Kornilov, G., L. Sidrevich, and J.W. Dippner, 2001. Fish and zooplankton interaction in the Central Baltic Sea. *ICES J. Mar. Science,* **58,** 579–588.

Liu, K-K., T-H, Peng, P-T, Shaw, F-K, Shiah, 2003. Circulation and biogeochemical processes in the East China Sea and the vicinity of Taiwan: an overview and a brif synthesis. *Prog. Oceanogr.,* **50,** 1055–1064.

Moll, A., and G. Radach, 2003. Review of three-dimensional ecological modeling related to the North Sea shelf system Part 1: Models and their results. *Progr. Oceanogr.,* **57,** 175–217.

Mollmann, C., G. Kornilovs, and L. Sidrevich, 2000. Long-term dynamics of main zooplankton species in the central Baltic Sea. *J. Plankton Res.,* **22,** 2015–2038.

Oguz, T., and J. W. Dippner, (in press). W. Climatic Regulation of the Black Sea ecosystem at interannual-to-decadal time scales Deep Sea Res. II.

PICES Report, 2003. PICES-GLOBEC International Program on Climate change and carrying capacity. The BASS/MODEL Report on trophic models of the Subarctic Pacific basin ecosystems. PICES Secretariat, Institute of Ocean Sciences, Sidney, British Columbia, Canada.

PICES Report, 2004. PICES Report on Marine Ecosystems of the North Pacific. Pre-publication of the North Pacific Marine Science Organization, PICES Secretariat, North Saanich, British Columbia, Canada.

Rebstock, G.A., and Y. S. Kang, 2003. A comparision of three marine ecosystems surrounding the Korean Peninsula: Responses to climate change. *Progr. Oceanogr.,* **59,** 357–379.

Simpson, J.H., J. Sharples & T. P. Rippeth, 1991. A prescriptive model of stratification induced by freshwater runoff. *Estuarine, Coastal and Shelf Science,* **33,** 23–35.

Yamanaka, Y., N. Yoshie, M. Fnoguchi, and M.J. Kishi, (2004). An ecosystem model coupled with nitrogen-silicon-carbon cycles applied to Station A-7 in the Northwestern Pacific. *J. Oceanogr.* **60,** 227–241.